Published on 26 November 2015. Downloaded by University of Science and Technology of China on 01/03/2016 13:30:13.

Green Chemistry

COMMUNICATION

View Article Online
View Journal | View Issue

Cite this: *Green Chem.*, 2016, **18**, 1212

Received 22nd October 2015,
Accepted 26th November 2015

DOI: 10.1039/c5gc02530c

www.rsc.org/greenchem

Palladium nanoparticles stabilized with N-doped porous carbons derived from metal–organic frameworks for selective catalysis in biofuel upgrade: the role of catalyst wettability†

Yu-Zhen Chen,[a] Guorui Cai,[a] Yanmei Wang,[b] Qiang Xu,[c] Shu-Hong Yu[a] and Hai-Long Jiang*[a]

Palladium nanoparticles were firstly stabilized with metal–organic framework-derived porous carbon for biofuel upgrade, where the catalyst wettability is crucial. The remarkable catalytic performance of Pd/NPC-ZIF-8 in water can be attributed to the well-dispersed and electron-rich Pd sites, high surface area and hierarchical pores, as well as the favorable hydrophilicity of NPC-ZIF-8.

In recent years, biofuels derived from the pyrolysis of lignocellulosic biomass have attracted considerable attention as a substitute for reducing the dependence on fossil fuel sources.[1] Unfortunately, bio-oils have a low calorific value, immiscibility with conventional fuels and instability over time, owing to high amounts of oxygen components involved. Therefore, bio-oils must be upgraded for oxygen removal if they would be fully used.[2] There are generally several approaches for bio-oil upgrading to a liquid transportation fuel, among which an effective and economic route is hydrodeoxygenation (HDO). However, the hydrophilic groups involved in the unprocessed biofuels make them hardly undergo HDO over traditional catalysts such as Pd/C. Recently, some novel catalysts have been developed to be effective, while they catalyze the reaction under harsh reaction conditions, such as high temperature (over 100 °C) or high pressure (1.0 MPa).[3] Moreover, the reports have demonstrated that sufficient contact between catalyst and substrates is necessary.[3] Therefore, the development of hydrophilic catalysts, which are wettable to the bio-oils and able to catalyze the biofuel upgrade with high activity and selectivity under mild conditions, is highly desired.

On the other hand, metal–organic frameworks (MOFs), as a relatively new class of porous materials, have attracted intense attention in recent two decades.[4–8] Recently, MOFs have been recognized to be ideal sacrificial templates to afford porous carbons *via* facile pyrolysis.[9] MOF-derived porous carbons possess great merits, such as tailorable structure and porosity, high surface area, homogeneous heteroatom (N, S, *etc.*) doping, and so on. Therefore, the MOF-derived porous carbon should be an excellent support/host for metal NPs. However, although metal NPs stabilized with MOFs for catalysis have been extensively reported recently,[10] in sharp contrast, to the best of our knowledge, no effort has been made on metal NPs stabilized with MOF-derived carbons for heterogeneous catalysis. Many interesting issues remain unresolved on this topic. In particular, the tunable nitrogen dopant in the MOF-derived porous carbon would endow it with hydrophilicity, which, if being employed for biofuel upgrade, would be of great significance.

Bearing this in mind, a representative MOF, ZIF-8 ($Zn(mim)_2$, mim = 2-methylimidazole),[11] has been converted to hydrophilic N-doped porous carbon (simply as NPC-ZIF-8-*T*, *T* represents the pyrolysis temperature; *T* is hereafter omitted for concision when it is 900) with a surface area as high as 2184 $m^2\ g^{-1}$ *via* a facile one-step pyrolysis. Subsequently, a Pd precursor can be introduced into the NPC by an incipient-wetness impregnation method and then reduced to be tiny Pd NPs under a H_2/Ar atmosphere.[2c] Remarkably, the resultant Pd/NPC-ZIF-8 catalyst inherits the good hydrophilicity of NPC-ZIF-8 and thus greatly promotes the biofuel upgrade reaction (Scheme 1), because the reactant (vanillin) and intermediate (vanillin alcohol) are highly soluble in water, while the target product (2-methoxy-4-methylphenol) is much more soluble in the oil phase. Therefore, the hydrophilic substrates are readily adsorbed by the catalyst while the final products soluble in hydrocarbon solvents tend to desorb from the catalyst surface, avoiding the blockage of catalytically active sites. Taking advantage of this, the reaction is promoted smoothly.

[a]*Hefei National Laboratory for Physical Sciences at the Microscale, Key Laboratory of Soft Matter Chemistry, Chinese Academy of Sciences, Collaborative Innovation Center of Suzhou Nano Science and Technology, Department of Chemistry, University of Science and Technology of China, Hefei, Anhui 230026, P.R. China. E-mail: jianglab@ustc.edu.cn; Fax: +86-551-63607861; Tel: +86-551-63607861*
[b]*Department of Polymer Science and Engineering, University of Science and Technology of China, Hefei, Anhui 230026, P. R. China*
[c]*National Institute of Advanced Industrial Science and Technology (AIST), Ikeda, Osaka 563-8577, Japan*
†Electronic supplementary information (ESI) available. See DOI: 10.1039/c5gc02530c

This journal is © The Royal Society of Chemistry 2016

Published on 26 November 2015. Downloaded by University of Science and Technology of China on 01/03/2016 13:30:13.

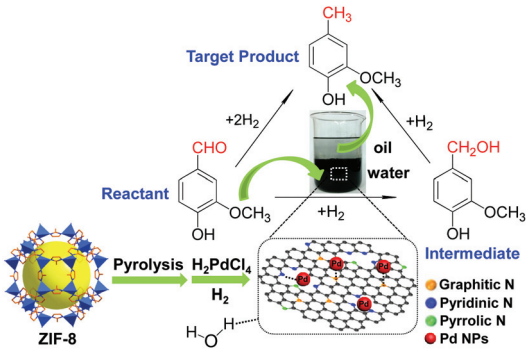

Scheme 1 Schematic illustration showing the synthetic strategy of ZIF-8-derived hydrophilic N-doped carbon and its selective catalysis in biofuel upgrade reaction.

A room-temperature reaction of $Zn(NO_3)_2$ and 2-methylimidazole facilely yielded uniform ZIF-8 nanocrystals with sizes of 50 nm (Fig. 1a; Experimental section, ESI†),[11c] which underwent pyrolysis at 900 °C under N_2 to afford N-doped porous carbon as the pyrolyzed ZnO was reduced by carbon to give evaporative Zn at such a high temperature.[9b] Delightedly, the obtained carbon particles are well dispersed without serious sintering and present a retained morphology and a bit reduced sizes of ZIF-8 nanocrystals, as demonstrated by scanning electron microscopy (SEM) observation (Fig. 1a and b). From the high resolution transmission electron microscopy (HRTEM) image, the apparent oriented multilayered domains and graphene sheets stacked in parallel are not readily distinguishable, whereas mostly disordered graphene layer domains are observed, indicating the relatively low graphitization degree (Fig. 1c). The elemental mapping indicates that the obtained NPC-ZIF-8 is mainly composed of carbon, and the element N is dispersed uniformly throughout the carbon matrix (Fig. 1d).

For comparison, the other two MOFs, ZIF-67 and MOF-5,[12] have also been synthesized and employed as precursors to afford porous carbons in the presence or absence of N atoms, which are denoted as NPC-ZIF-67 and C-MOF-5, respectively. The texture and porosity of the different MOFs before and after pyrolysis, commercial activated carbon (AC) and Pd/C, have been also characterized by the N_2 sorption measurement at 77 K (Fig. S1, ESI†). The original ZIF-8 and ZIF-67 show a typical microporous character with high surface areas (BET, 1718 and 1782 $m^2\ g^{-1}$, respectively) and large pore volumes. After pyrolysis, the BET surface areas for NPC-ZIF-8, NPC-ZIF-67 and C-MOF-5 are 2184, 573 and 2243 $m^2\ g^{-1}$, and pore volumes are 1.6, 0.34 and 1.9 $m^3\ g^{-1}$, respectively. It is found that the pyrolysis temperature significantly affects the BET surface area and pore character of the resultant carbons from ZIF-8 (Fig. S1b, ESI†). The relatively low BET surface area and pore volume for NPC-ZIF-67 are in agreement with the previous studies.[13] The IV-type N_2 sorption curves for the MOF-derived porous carbons reveal the presence of hierarchical micropores and mesopores, while commercial Pd/C and AC almost show the microporous character only, which can be verified by the pore size distribution (Fig. S2, ESI†).

The X-ray photoelectron spectroscopy (XPS) analysis for N 1s reveals that there are four types of nitrogen species: graphitic-N (N1, 401.1 ± 0.3 eV), pyrrolic-N (N2, 400.5 ± 0.3 eV), pyridinic-N (N3, 398.5 ± 0.2 eV) and oxidized nitrogen N^+–O^- (N4, 404.4 ± 0.1 eV) in all N-involved samples (Fig. 2a, S3 and Table S1, ESI†).[14] In both NPC-ZIF-8 and NPC-ZIF-67, the N1 peak is dominant, which might be because the graphitic-N is the most stable species in carbon at a high temperature (900 °C).[15] Additional nitrogen atoms have been introduced into the NPC-ZIF-8, C-MOF-5 and AC as far as possible, by using urea as a precursor to yield N-rich carbon materials NPC-ZIF-8-urea, C-MOF-5-urea and AC-urea, respectively. The

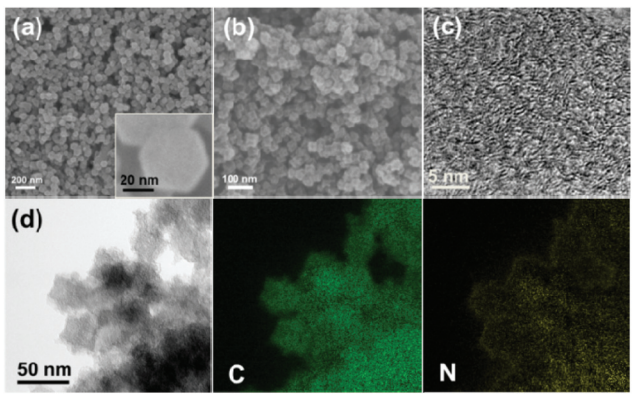

Fig. 1 SEM images of (a) ZIF-8 and (b) NPC-ZIF-8. (c) HRTEM image of NPC-ZIF-8. (d) TEM image and the corresponding elemental mapping showing the uniform dispersion of C and N. Inset in (a): enlarged single ZIF-8 particle.

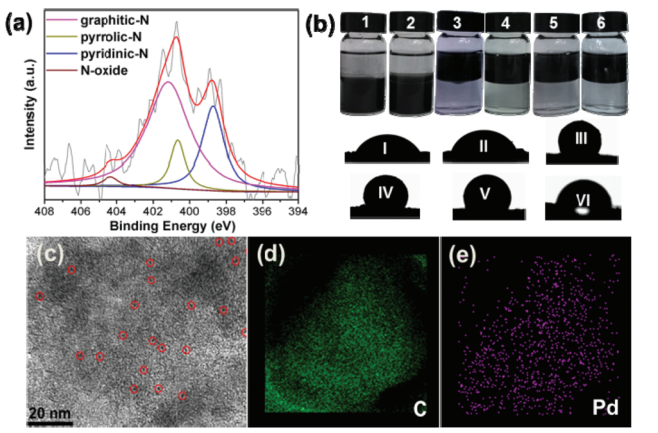

Fig. 2 (a) XPS spectra of N 1s for NPC-ZIF-8. (b) The wettability of NPC-ZIF-8 (1), NPC-ZIF-67 (2), AC (3), AC-urea (4), C-MOF-5 (5) and C-MOF-5-urea (6) in a biphasic solution, the organic upper (ethyl acetate) and the aqueous bottom (water), and their corresponding air–water contact angles for NPC-ZIF-8 (I), NPC-ZIF-67 (II), AC (III), AC-urea (IV), C-MOF-5 (V) and C-MOF-5-urea (VI). (c) TEM image for Pd/NPC-ZIF-8 (the ultrafine Pd NPs of ~1 nm size are highlighted with red circles) and the related element mappings for (d) C and (e) Pd.

Published on 26 November 2015. Downloaded by University of Science and Technology of China on 01/03/2016 13:30:13.

XPS data demonstrate that the nitrogen has been successfully doped into these carbon materials (Fig. S3, ESI†). Different from the *in situ* generated graphitic-N existed in NPC-ZIF-8 and NPC-ZIF-67, the newly introduced N species in the urea-treated carbon materials belong to other N forms (Table S1, ESI†), similar to a previous report.[16] The Raman spectra for NPC-ZIF-8, C-MOF-5 and AC indicate that the highest degree of graphitization for NPC-ZIF-8 with the lowest I_D/I_G value (Fig. S4a, ESI†), together with the HRTEM result mentioned above, suggesting the low graphitization for all these carbon materials. In addition, the better of graphitization of NPC-ZIF-8 can be obtained with increasing pyrolysis temperatures (Fig. S4b, ESI†).

In order to investigate the hydrophilicity/hydrophobicity nature of the obtained carbon materials, all the samples were dispersed at the interface of a biphasic solution, in which the upper part was ethyl acetate and the bottom was water (Fig. 2b, top). Interestingly, the NPC-ZIF-8 and NPC-ZIF-67 can be well dispersed in water, indicating that they are well wettable and hydrophilic. On the contrary, the N-free AC and C-MOF-5 stay in the organic phase only. Although the urea treatment makes the N contents in the resultant AC-urea and C-MOF-5-urea even higher than that in NPC-ZIF-8, as suggested by elemental analysis (Table S2, ESI†), their wettability to water has only a small change. As a result, they are still dispersed in the organic phase, revealing the retained hydrophobicity. The phenomenon is supported by the results of contact angles, which display that the air–water contact angles on the surface of NPC-ZIF-8, NPC-ZIF-67, AC, AC-urea, C-MOF-5 and C-MOF-5-urea are 50°, 59°, 125°, 116°, 119° and 85°, respectively (Fig. 2b, bottom). The above results indicate that the hydrophobicity may be related to the N existence form: the N1 species plays an important role while other species have a relatively small effect on their wettability.[3b] It is proposed that the permanent polarization occurs between graphitic-N and adjacent C due to their significant difference in the electronegativity (Pauling scale of N: 3.04; Pauling scale of C: 2.55). As a result, the changed charge distribution of graphitic N species facilitates their interaction with nucleophilic H_2O molecules. In comparison, pyridinic-N and pyrrolic-N have lone-pair electrons in the catalyst and are not favorable for the adsorption of H_2O molecules.[17]

Given the highly porous and great hydrophilic nature, NPC-ZIF-8 might be suitable for stabilizing small Pd NPs with inherited hydrophilicity, which would be miscible with unprocessed biofuels, and thus ideal for catalyzing their upgrade. Therefore, the obtained carbon materials and commercial metal oxides (TiO_2, SiO_2 and Al_2O_3) were utilized as supports/hosts to load Pd NPs by a simple incipient-wetness impregnation method. The actual contents of Pd NPs in all catalysts were evaluated by inductively coupled plasma atomic emission spectrometry (ICP-AES) (Table S3, ESI†). The powder X-ray diffraction (XRD) profiles show a broad graphitic stacking peak at ~24.0°, but no diffraction peak for Pd NPs can be detected in Pd/NPC-ZIF-8, revealing that the Pd NPs could be very small (Fig. S5, ESI†). The assumption is consistent with the results of TEM observation, which present the highly dispersed and ultrafine Pd NPs with sizes of ~1 nm or even less (Fig. 2c and S6a, ESI†). It is assumed that the hydrophilic micropores (1–2 nm) and nitrogen species in NPC-ZIF-8 are favorable to stabilize and avoid the aggregation of Pd NPs. The elemental mapping for Pd/NPC-ZIF-8 further verify the highly homogeneous dispersion of Pd NPs in the carbon matrix (Fig. 2d, e and S6c, d, ESI†). As expected, the wettability of MOF-derived porous carbons is well retained upon loading Pd NPs (Fig. S7 and S8, ESI†).

Encouraged by the above results, the HDO of vanillin in aqueous solution was investigated as a model catalytic reaction for biofuel upgrade over the obtained Pd catalysts (Table 1). There are two products, *i.e.* 2-methoxy-4-methylphenol (**A**, main product) and vanillin alcohol (**B**, intermedium) produced during the HDO of vanillin under mild conditions.

Table 1 Nanoporous-hydrophilic N-doped carbon supported Pd nanoparticle catalysts for hydrodeoxygenation of vanillin in aqueous solution[a]

						Sel.[b] (%)	
Entry	Catalyst	S_{BET} ($m^2\ g^{-1}$)	Time (h)	Con.[b] (%)	TOF[c] (h^{-1})	**B**	
1	Pd/NPC-ZIF-8	2184	2	100	100	0	100
2	Pd/ZIF-8-urea	2178	2	100	93	10	90
3	Pd/NPC-ZIF-67	573	2	99	54	30	70
4	Pd/C-MOF-5	2243	3	60	36	2	98
5	Pd/C-MOF-5-urea	1700	3	99	78	1	99
6	Pd/AC	1856	3	36	22	0	100
7	Pd/AC-urea	1990	3	58	20	19	81
8	Pd/C	925	5	98	15	38	62
9	Pd/TiO_2	50	3	99	64	16	84
10	Pd/SiO_2	309	3	11	4	25	75
11	Pd/γ-Al_2O_3	3	3	14	3.4	54	46
12	NPC-ZIF-8	2184	3	—	—	—	—
13	No	—	—	—	—	—	—

[a] Reaction conditions: vanillin (89 mg, 0.585 mmol), catalyst (50 mg), S/C (molar ratio of substrate/metal) = 208, water (3 mL), H_2 (0.2 MPa), 90 °C. [b] Conversion and selectivity were analyzed by GC. [c] Calculated based on the target product.

 This journal is © The Royal Society of Chemistry 2016

Published on 26 November 2015. Downloaded by University of Science and Technology of China on 01/03/2016 13:30:13.

Among the diverse Pd catalysts investigated, the Pd/NPC-ZIF-8 possesses the best catalytic conversion (100%) and selectivity (100%) to the target product 2-methoxy-4-methylphenol (**A**, completed in 2 h at 0.2 MPa H_2, 90 °C) in the HDO reaction of vanillin (entry 1, Fig. S9, ESI†). Pd/NPC-ZIF-67 led to 99% conversion and 70% selectivity towards target **A** after 2 h (entry 3), and Pd/C-MOF-5 only converted 60% after a 3 h reaction (entry 4) under identical experimental conditions. In contrast, the activity was greatly improved and the reaction almost completed within the given time over C-MOF-5-urea in the presence of the N dopant under the same conditions (entry 5). The phenomenon was also observed for Pd/AC and Pd/AC-urea (entries 6 and 7), inferring that the N dopant for the original N-free catalysts played a critical role in the reaction. Unexpectedly, when Pd/NPC-ZIF-8-urea with higher N contents was used, its activity was even inferior to that of Pd/NPC-ZIF-8 (entry 2), indicating that the high N content may not necessarily exert a positive effect on the catalytic activity. Taking the above results together with the contact angles of these catalysts, the wettability change should account for the activity improvement: compared to the original carbons, the lower contact angles of urea-treated C-MOF-5-urea and Pd/AC-urea result in their higher activity; the similar hydrophilicity of Pd/NPC-ZIF-8 before and after urea treatment well explains the almost unaltered catalytic activities. For comparison, commercial Pd/C as well as metal oxide-supported Pd NP catalysts, including Pd/TiO_2, Pd/SiO_2 and Pd/γ-Al_2O_3, were also examined for the catalytic reaction and all these catalysts exhibited relatively low activities (entries 8–11), possibly due to their poor wettability, low mass transfer of the hydrophilic substrate (for Pd/C), and the low surface area and large Pd NPs (for Pd/metal oxide, Fig. S10, ESI†).

In addition, the reaction was also conducted with Pd/NPC-ZIF-8 at different temperatures (70–110 °C) (Table S4, ESI†). The results unambiguously display that the higher reaction temperature leads to much faster reaction kinetics. Moreover, compared with the previously reported Pd/SWNT-SiO_2, Pd@$CN_{0.132}$ and Pd/MSMF catalysts that complete the reaction under relatively high temperature and pressure conditions,[3a–c] the Pd/NPC-ZIF-8 catalyst exhibits superb catalytic activity and selectivity for hydrodeoxygenation of vanillin in 2 hours under mild conditions (90 °C, 0.2 MPa H_2). Even under the conditions of 90 °C and 0.1 MPa H_2, the reaction is able to show a satisfactory activity (100% conversion, 95% selectivity) in 10 h in the presence of the Pd/NPC-ZIF-8 catalyst (Fig. S11, ESI†). It is proposed that the hydrophilicity of Pd/NPC-ZIF-8 is mostly responsible for the excellent activity, while for ultrafine Pd NPs, high surface area and porosity involved in the catalyst also play indispensable roles.

It is found that the pyrolysis temperature (T = 600, 700, 800, 900, 1000 °C) of ZIF-8 has significant effects on the catalytic performance of Pd/NPC-ZIF-8-T for the HDO of vanillin although these catalysts have similar hydrophilicity and contact angles (Fig. S12, ESI†). The results indicate that 900 °C is an optimal temperature for pyrolysis and Pd/NPC-ZIF-8-900

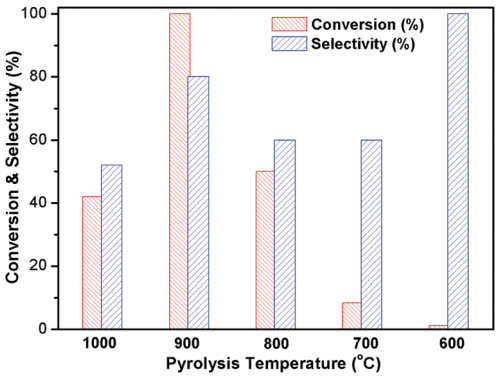

Fig. 3 The catalytic activity for the HDO of vanillin at the same reaction time (1 h) based on Pd/NPC-ZIF-8 with different pyrolysis temperatures of ZIF-8. Reaction conditions: vanillin (89 mg, 0.585 mmol), 0.6% Pd/NPC-ZIF-8 (50 mg), S/C (molar ratio of the substrate/metal) = 208, water (3 mL), H_2 (0.2 MPa), 90 °C.

completed the reaction and showed selectivity (80%) in 1 h with a rapid kinetics and a high TOF of 160 h^{-1} (Fig. 3), surpassing all reported catalysts under similar conditions (Table S5†). The good activity of Pd/NPC-ZIF-8-900 is not only due to its hydrophilicity, the high content of graphitic-N and high surface area, but also due to the electron-rich Pd, resulting from the strong interaction between Pd and graphitic-N and electron transfer from graphitic-N to Pd,[18] which would be largely beneficial to the activity. The existing electron transfer was further confirmed by the XPS data. The 3d peaks for Pd(0) shift gradually to lower binding energies along with increasing pyrolysis temperatures (700–900 °C) for ZIF-8 (Fig. S13, ESI†), indicating that significant electron transfer occurs from graphitic-N to Pd in Pd/NPC-ZIF-8-900. We have also proposed the primary reaction mechanism as follows: at the initial stage of the reaction, vanillin is readily adsorbed onto the hydrophilic surface of the catalyst, and H_2 is activated by the electronically supported Pd. The C=O bond is then mainly hydrogenated and deoxidized to the main product. The residue was hydrogenated to the vanillin alcohol (intermedium) first and further converted to the final product by hydrogenolysis (Scheme 2).[19] The final product with hydrophobicity leaves the catalyst surface quickly, being replaced by a more strongly binding hydrophilic reactant.

In addition, as a heterogeneous catalyst, Pd/NPC-ZIF-8 can be readily separated from the reaction solution by simple filtration. A slight decrease during the recycling experiment

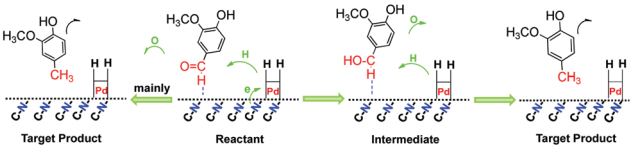

Scheme 2 Proposed reaction mechanism of HDO of vanillin in aqueous solution over Pd/NPC-ZIF-8.

Published on 26 November 2015. Downloaded by University of Science and Technology of China on 01/03/2016 13:30:13.

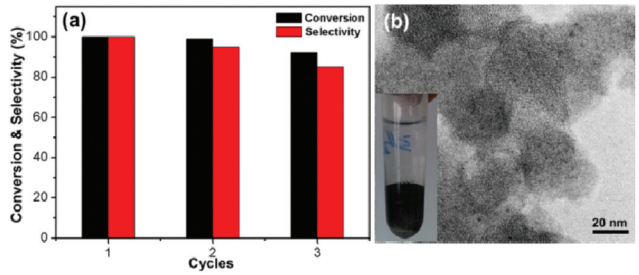

Fig. 4 (a) Recycling performance for the conversion of vanillin and selectivity to the target product A after the three cycles over the Pd/NPC-ZIF-8 catalyst. (b) A representative TEM image of the recycled Pd/NPC-ZIF-8 catalyst after 3 runs (inset shows the separation of the catalyst and reactant/product by simple extraction with ethyl acetate).

was observed, which might be due to the slight leaching of the Pd NPs and a little bit aggregation of Pd NPs, as shown by a representative TEM image of Pd/NPC-ZIF-8 after 3 runs of reaction, where small Pd NPs become almost observable (Fig. 4). Despite this, no identifiable peak for Pd in the PXRD pattern after 3 catalytic cycles reveals the almost nonexistence of large Pd NPs (Fig. S5b, ESI†).

In summary, diverse MOFs have been converted to porous carbons with different degrees of hydrophilicity at different pyrolysis temperatures, which were employed to stabilize Pd NPs for catalysis in bio-oil refining. It is found that the wettability of MOF-derived porous carbons plays a crucial role in the catalytic activity of biofuel upgrade. The Pd NPs stabilized with NPC-ZIF-8 with great hydrophilicity exhibit excellent catalytic performance for the HDO of vanillin, a common component in lignin-derived bio-oil, under mild conditions in a green solvent, water. The remarkable catalytic activity, selectivity and recyclability of Pd/NPC-ZIF-8 can be mainly attributed to the following: (1) the high surface area and hierarchical pores involved in the catalyst not only enable the stabilization of Pd NPs in very small sizes (~1 nm) but also facilitate the transport of reactants and products; (2) the high content of graphitic-N doping merits the great hydrophilicity, which ensures the sufficient contact between substrates and catalyst; (3) the graphitic-N in the carbon favors the electron transfer to Pd sites and the resultant electron-rich Pd greatly improves the catalytic activity; (4) the high stability of NPC-ZIF-8 evidently is also helpful to the recyclability. Given the structural diversity and tailorability of MOFs, there is a huge opportunity to achieve MOF-derived porous carbons with great tunability of properties such as structure, component, porosity, pore size, surface area, *etc.*, which would open a new avenue to carbon supported metal NPs in catalysis.

This work was supported by the NSFC (21371162, 51301159 and 21521001), the 973 program (2014CB931803), the NSF of Anhui Province (1408085MB23), the Research Fund for the Doctoral Program of Higher Education of China (20133402120020), the Recruitment Program of Global Youth Experts and the Fundamental Research Funds for the Central Universities (WK2060190026).

Notes and references

1 (*a*) D. Tilman, J. Hill and C. Lehman, *Science*, 2006, **314**, 1598–1600; (*b*) V. G. W. Huber, S. Iborra and A. Corma, *Chem. Rev.*, 2006, **106**, 4044–4049; (*c*) C. Luo, S. Wang and H. Liu, *Angew. Chem., Int. Ed.*, 2007, **46**, 7636–7639; (*d*) G. W. Huber and A. Corma, *Angew. Chem., Int. Ed.*, 2007, **46**, 7184–7201; (*e*) E. M. Rubin, *Nature*, 2008, **454**, 841–845; (*f*) H. Olcay, A. V. Subrahmanyam, R. Xing, J. Lajoie, J. A. Dumesic and G. W. Huber, *Energy Environ. Sci.*, 2013, **6**, 205–216.

2 (*a*) M. Stöcker, *Angew. Chem., Int. Ed.*, 2008, **47**, 9200–9211; (*b*) P. M. Mortensen, J.-D. Grunwaldt, P. A. Jensen, K. G. Knudsen and A. D. Jensen, *Appl. Catal., A*, 2011, **407**, 1–19; (*c*) K. Yana, T. Lafleur, G. Wua, J. Liao, C. Cenga and X. Xie, *Appl. Catal., A*, 2013, **468**, 52–58; (*d*) M. Saidi, F. Samimi, D. Karimipourfard, T. Nimmanwudipong, B. C. Gates and M. R. Rahimpour, *Energy Environ. Sci.*, 2014, **7**, 103–129; (*e*) K. Yan, T. Lafleur, X. Wu, J. Chai, G. Wu and X. Xie, *Chem. Commun.*, 2015, **51**, 6984–6987.

3 (*a*) S. Crossley, J. Faria, M. Shen and D. E. Resasco, *Science*, 2010, **327**, 68–72; (*b*) X. Xu, Y. Li, Y. Gong, P. Zhang, H. Li and Y. Wang, *J. Am. Chem. Soc.*, 2012, **134**, 16987–16990; (*c*) Z. Lv, Q. Sun, X. Meng and F.-S. Xiao, *J. Mater. Chem. A*, 2013, **1**, 8630–8635; (*d*) X. Yang, Y. Liang, X. Zhao, Y. Song, L. Hu, X. Wang, Z. Wang and J. Qiu, *RSC Adv.*, 2014, **4**, 31932–31936; (*e*) Z. Zhu, H. Tan, J. Wang, S. Yu and K. Zhou, *Green Chem.*, 2014, **16**, 2636–2643; (*f*) A. Aijaz, Q.-L. Zhu, N. Tsumori, T. Akita and Q. Xu, *Chem. Commun.*, 2015, **51**, 2577–2580.

4 (*a*) J. R. Long and O. M. Yaghi, *Chem. Soc. Rev.*, 2009, **38**, 1213–1214; (*b*) H.-C. Zhou, J. R. Long and O. M. Yaghi, *Chem. Rev.*, 2012, **112**, 673–674; (*c*) H. Furukawa, K. E. Cordova, M. O'Keeffe and O. M. Yaghi, *Science*, 2013, **341**, 974–986; (*d*) H.-C. Zhou and S. Kitagawa, *Chem. Soc. Rev.*, 2014, **43**, 5415–5418.

5 (*a*) J. Liu, P. K. Thallapally, B. P. McGrail, D. R. Brown and J. Liu, *Chem. Soc. Rev.*, 2012, **41**, 2308–2322; (*b*) K. Sumida, D. L. Rogow, J. A. Mason, T. M. McDonald, E. D. Bloch, Z. R. Herm, T.-H. Bae and J. R. Long, *Chem. Rev.*, 2012, **112**, 724–781; (*c*) M. P. Suh, H. J. Park, T. K. Prasad and D.-W. Lim, *Chem. Rev.*, 2012, **112**, 782–835; (*d*) P. Nugent, Y. Belmabkhout, S. D. Burd, A. J. Cairns, R. Luebke, K. Forrest, T. Pham, S. Ma, M. Eddaoudi and M. J. Zaworotko, *Nature*, 2013, **495**, 80–84; (*e*) J.-R. Li, J. Sculley and H.-C. Zhou, *Chem. Rev.*, 2012, **112**, 869–932; (*f*) Y. He, W. Zhou, G. Qian and B. Chen, *Chem. Soc. Rev.*, 2014, **43**, 5657–5678; (*g*) A. J. Brown, N. A. Brunelli, K. Eum, F. Rashidi, J. R. Johnson, W. J. Koros, C. W. Jones and S. Nair, *Science*, 2014, **345**, 72–75.

6 (*a*) D. Farrusseng, S. Aguado and C. Pinel, *Angew. Chem., Int. Ed.*, 2009, **48**, 7502–7513; (*b*) A. Corma, H. García and F. X. Llabrés i Xamena, *Chem. Rev.*, 2010, **110**, 4606–4655; (*c*) H.-L. Jiang and Q. Xu, *Chem. Commun.*, 2011, **47**, 3351–3370; (*d*) J. Gascon, A. Corma, F. Kapteijn and F. X. Llabrés i Xamena, *ACS Catal.*, 2014, **4**, 361–378; (*e*) T. Zhang and

 This journal is © The Royal Society of Chemistry 2016

Published on 26 November 2015. Downloaded by University of Science and Technology of China on 01/03/2016 13:30:13.

W. Lin, *Chem. Soc. Rev.*, 2014, **43**, 5982–5993; (*f*) J. Liu, L. Chen, H. Cui, J. Zhang, L. Zhang and C.-Y. Su, *Chem. Soc. Rev.*, 2014, **43**, 6011–6061; (*g*) G. Huang, Y.-Z. Chen and H.-L. Jiang, *Acta Chim. Sin.*, 2015, DOI: 10.6023/A15080547.

7 (*a*) B. Chen, S. Xiang and G. Qian, *Acc. Chem. Res.*, 2010, **43**, 1115–1124; (*b*) Y. Takashima, V. Martinez, S. Furukawa, M. Kondo, S. Shimomura, H. Uehara, M. Nakahama, K. Sugimoto and S. Kitagawa, *Nat. Commun.*, 2011, **2**, 168–175; (*c*) L. E. Kreno, K. Leong, O. K. Farha, M. Allendorf, R. P. Van Duyne and J. T. Hupp, *Chem. Rev.*, 2012, **112**, 1105–1125; (*d*) R.-B. Lin, F. Li, S.-Y. Liu, X.-L. Qi, J.-P. Zhang and X.-M. Chen, *Angew. Chem., Int. Ed.*, 2013, **52**, 13429–13433; (*e*) Z. Hu, B. J. Deibert and J. Li, *Chem. Soc. Rev.*, 2014, **43**, 5815–5840.

8 (*a*) Z. Wang and S. M. Cohen, *Chem. Soc. Rev.*, 2009, **38**, 1315–1329; (*b*) J. An, S. J. Geib and N. L. Rosi, *J. Am. Chem. Soc.*, 2009, **131**, 8376–8377; (*c*) A. Mallick, B. Garai, D. D. Díaz and R. Banerjee, *Angew. Chem., Int. Ed.*, 2013, **52**, 13755–13759; (*d*) H. Kitagawa, *Nat. Chem.*, 2009, **1**, 689–690; (*e*) T. K. Kim, K. J. Lee, J. Y. Cheon, J. H. Lee, S. H. Joo and H. R. Moon, *J. Am. Chem. Soc.*, 2013, **135**, 8940–8946.

9 (*a*) B. Liu, H. Shioyama, T. Akita and Q. Xu, *J. Am. Chem. Soc.*, 2008, **130**, 5390–5391; (*b*) H.-L. Jiang, B. Liu, Y. Q. Lan, K. Kuratani, T. Akita, H. Shioyama, F. Zong and Q. Xu, *J. Am. Chem. Soc.*, 2011, **133**, 11854–11857; (*c*) A. Almasoudi and R. Mokaya, *J. Mater. Chem.*, 2012, **22**, 146–152; (*d*) D. Zhao, J.-L. Shui, L. R. Grabstanowicz, C. Chen, S. M. Commet, T. Xu, J. Lu and D.-J. Liu, *Adv. Mater.*, 2014, **26**, 1093–1097; (*e*) P. Zhang, F. Sun, Z. Xiang, Z. Shen, J. Yun and D. Cao, *Energy Environ. Sci.*, 2014, **7**, 442–450; (*f*) G. Srinivas, V. Krungleviciute, Z.-X. Guo and T. Yildirim, *Energy Environ. Sci.*, 2014, **7**, 335–342; (*g*) J. Tang, R. R. Salunkhe, J. Liu, N. L. Torad, M. Imura, S. Furukawa and Y. Yamauchi, *J. Am. Chem. Soc.*, 2015, **137**, 1572–1580; (*h*) Y.-Z. Chen, C. Wang, Z.-Y. Wu, Y. Xiong, Q. Xu, S.-H. Yu and H.-L. Jiang, *Adv. Mater.*, 2015, **27**, 5010–5016.

10 (*a*) S. Hermes, M.-K. Schröter, R. Schmid, L. Khodeir, M. Muhler, A. Tissler, R. W. Fischer and R. A. Fischer, *Angew. Chem., Int. Ed.*, 2005, **44**, 6237–6241; (*b*) H. R. Moon, J. H. Kim and M. P. Suh, *Angew. Chem., Int. Ed.*, 2005, **44**, 1261–1265; (*c*) Y. K. Hwang, D. Y. Hong, J. S. Chang, S. H. Jhung, Y. K. Seo, J. Kim, A. Vimont, M. Daturi, C. Serre and G. Férey, *Angew. Chem., Int. Ed.*, 2008, **47**, 4144–4148; (*d*) T. Ishida, M. Nagaoka, T. Akita and M. Haruta, *Chem. – Eur. J.*, 2008, **14**, 8456–8460; (*e*) H.-L. Jiang, B. Liu, T. Akita, M. Haruta, H. Sakurai and Q. Xu, *J. Am. Chem. Soc.*, 2009, **131**, 11302–11303; (*f*) B. Yuan, Y. Pan, Y. Li, B. Yin and H. Jiang, *Angew. Chem., Int. Ed.*, 2010, **49**, 4054–4058; (*g*) G. Lu, S. Li, Z. Guo, O. K. Farha, B. G. Hauser, X. Qi, Y. Wang, X. Wang, S. Han, X. Liu, J. S. DuChene, H. Zhang, Q. Zhang, X. Chen, J. Ma, S. C. J. Loo, W. D. Wei, Y. Yang, T. J. Hupp and F. Huo, *Nat. Chem.*, 2012, **4**, 310; (*h*) C. H. Kuo, Y. Tang, L. Y. Chou, B. T. Sneed, C. N. Brodsky, Z. P. Zhao and C.-K. Tsung, *J. Am. Chem. Soc.*, 2012, **134**, 14345–14348; (*i*) J. Long, H. Liu, S. Wu, S. Liao and Y. Li, *ACS Catal.*, 2013, **3**, 647–654; (*j*) Z. Zhang, Y. Chen, X. Xu, J. Zhang, G. Xiang, W. He and X. Wang, *Angew. Chem., Int. Ed.*, 2014, **53**, 429–433; (*k*) X. Li, Z. Guo, C. Xiao, T. W. Goh, D. Tesfagaber and W. Huang, *ACS Catal.*, 2014, **4**, 3490–3497; (*l*) M. Zhao, K. Deng, L. He, Y. Liu, G. Li, H. Zhao and Z. Tang, *J. Am. Chem. Soc.*, 2014, **136**, 1738–1741; (*m*) Y.-Z. Chen, Y.-X. Zhou, H. Wang, J. Lu, T. Uchida, Q. Xu, S.-H. Yu and H.-L. Jiang, *ACS Catal.*, 2015, **5**, 2062–2069; (*n*) Y.-Z. Chen, L. Liang, Q. Yang, M. Hong, Q. Xu, S.-H. Yu and H.-L. Jiang, *Mater. Horiz.*, 2015, **2**, 606–612.

11 (*a*) K. S. Park, Z. Ni, A. P. Côté, J. Y. Choi, R. Huang, F. J. Uribe-Romo, H. K. Chae, M. O'Keeffe and O. M. Yaghi, *Proc. Natl. Acad. Sci. U. S. A.*, 2006, **103**, 10186–10191; (*b*) X.-C. Huang, Y.-Y. Lin, J.-P. Zhang and X.-M. Chen, *Angew. Chem., Int. Ed.*, 2006, **45**, 1557–1559; (*c*) S. R. Venna, J. B. Jasinski and M. A. Carreon, *J. Am. Chem. Soc.*, 2010, **132**, 18030–18033.

12 (*a*) D. J. Tranchemontagne, J. R. Hunt and O. M. Yaghi, *Tetrahedron*, 2008, **64**, 8553–8557; (*b*) J. Qian, F. Sun and L. Qin, *Mater. Lett.*, 2012, **82**, 220–223.

13 (*a*) N. L. Torad, M. Hu, S. Ishihara, H. Sukegawa, A. Belik, M. Imura, K. Ariga, Y. Sakka and Y. Yamauchi, *Small*, 2014, **10**, 2096; (*b*) X. Wang, J. Zhou, H. Fu, W. Li, X. Fan, G. Xin, J. Zheng and X. Li, *J. Mater. Chem. A*, 2014, **2**, 14064–14070.

14 (*a*) P. H. Matter, L. Zhang and U. S. Ozkan, *J. Catal.*, 2006, **239**, 83–96; (*b*) G. Wu, M. Nelson, S. Ma, H. Meng, G. Cui and P. K. Shen, *Carbon*, 2011, **49**, 3972–3982; (*c*) Z. Li, Z. Xu, X. Tan, H. Wang, C. M. B. Holt, T. Stephenson, B. C. Olsen and D. Mitlin, *Energy Environ. Sci.*, 2013, **6**, 871–878.

15 J. R. Pels, F. Kapteijn, J. A. Moulijn and Q. Zhu, *Carbon*, 1995, **33**, 1641–1653.

16 L.-F. Chen, Z.-H. Huang, H.-W. Liang, Q.-F. Guan and S.-H. Yu, *Adv. Mater.*, 2013, **25**, 4746–4752.

17 W. J. Lee, U. N. Maiti, J. M. Lee, J. Lim, T. H. Han and S. O. Kim, *Chem. Commun.*, 2014, **50**, 6818–6830.

18 X. Ning, H. Yu, F. Peng and H. Wang, *J. Catal.*, 2015, **325**, 136.

19 (*a*) Y. Wang, J. Yao, H. Li, D. Su and M. Antonietti, *J. Am. Chem. Soc.*, 2011, **133**, 2362–2365; (*b*) X.-H. Li and M. Antonietti, *Chem. Soc. Rev.*, 2013, **42**, 6593–6604.